

# A photoluminescent molecular host with aggregation-induced emission enhancement, multi-stimuli responsive properties and tunable photoluminescence host-guest interaction in the solid state

Hamideh Nikookar, Parviz Rashidi-Ranjbar\*

School Of Chemistry, College of Science, University of Tehran, Tehran, Iran

## ARTICLE INFO

### Keywords:

Photoluminescence  
Aggregation-induced emission enhancement  
Stimuli-responsive  
Host-guest interactions  
Pi-Pi interactions

## ABSTRACT

The development of controllable multimodal luminescent materials that are responsive to external stimuli has been a challenge. In this study, a photoluminescent (PL) molecular host with aggregation-induced emission enhancement (AIEE) characteristic and multi-stimuli responsive properties has been designed, synthesized and its fluorescence response to mechanical, thermal, anion and guest stimuli have been studied in the solid state. Host 1 displays reversible tricolor-changing PL triggered by mechanical and thermal stimulations. Furthermore, anion exchange has demonstrated that the emission is affected by the anion size and the affinity between cation and anion moieties, resulting in enhancement or quenching effects. Additionally, grinding was used for inclusion of guests in the host molecular packing to tune the PL properties, most probably due to  $\pi$ - $\pi$  interactions between molecular host and aromatic guests.

## 1. Introduction

The stimuli-responsive materials are highly interested because of their applications in memory, sensors, bio-imaging, and displays [1]. A wide variety of external stimuli which induce changes in chemical and physical properties of materials have been reported, such as electric current [2], irradiation, [3] aggregation [4], solvent polarity [5], temperature [6], mechanical force [7], pH [8] and organic solvent vapor [9].

Although the dichromic fluorescent systems have been successfully developed in the solid state [10], there are few examples of materials that display multicolor PL with stimuli. [11] Such an extent of various applications in diverse fields enforces researchers to design new compounds as single molecules [12], polymers [13], metal-organic frameworks [14], quantum dots [15] and nanoparticles [16] which provide tunable multicolor emission in solution or solid state.

On the other hands, noncovalent interactions in host-guest complexes display excellent strategy to modify chemo-physical properties of materials and provide color spectra through adjustment of emission light [17]. Hydrogen bonding, metal-ligand coordination, and  $\pi$ - $\pi$  stacking interactions have been reported in PL tunable systems [18],  $\pi$ - $\pi$  interactions are facile, non-destructive and particularly promising for applications from material science to molecular biology such as nucleic acids sequencing, protein folding, biosensors, crystal packing,

and drug delivery [19].  $\pi$ - $\pi$  interactions not only lessen solubility of organic compounds but also induce ACQ effect in luminogenic molecules resulting in significant fluorescence intensity and quantum yield decrease in solution or solid state that limits their applications. This phenomenon occurs when the aromatic sheets accumulate in stack form, and the excited states of aggregates often relax via non-radiative pathways [4d]. Various approaches have been developed to prevail with the ACQ effect in  $\pi$ -conjugated systems. For example, branched chains [20], bulky cyclics [21], spiro kinks [22], and dendritic wedges [23] have been attached to aromatic rings. This strategy led to the discovery of aggregation-induced emission (AIE) or aggregation-induced emission enhancement (AIEE) materials that are non-emissive or weak emissive in dilute solution and strong emissive in aggregated forms [24]. The engineering of  $\pi$ - $\pi$  interaction systems pursue good solvation, high quantum yield, good charge transfer (CT), and other optoelectronic properties.

The development of supramolecular systems with host-guest interactions to design color-tunable luminogens based on the modification of core fluorophores is challenging [25]. However, there have been a few reports [26] of the host-guest systems such as cyclodextrin or cucurbit [8] uril that display multicolor PL due to interactions with a fluorescent guest molecule. Traditionally, solution-phase crystallization has been used to form inclusion compounds in supramolecular chemistry. However, it is difficult to find an appropriate solvent for co-crystallization of

\* Corresponding author.

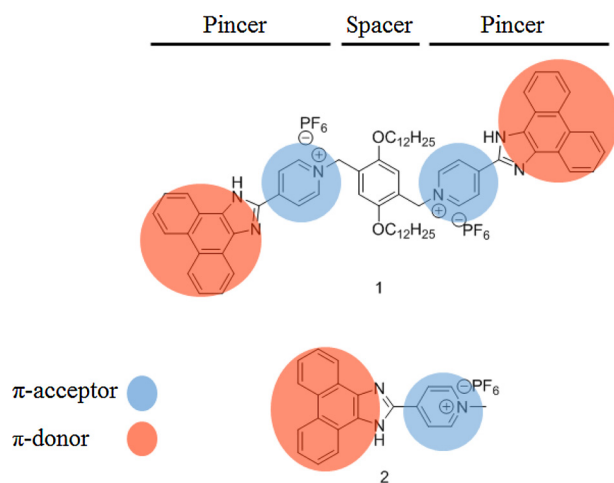
E-mail address: [parvizrashidi2@ut.ac.ir](mailto:parvizrashidi2@ut.ac.ir) (P. Rashidi-Ranjbar).

<https://doi.org/10.1016/j.jphotochem.2019.112106>

Received 9 May 2019; Received in revised form 22 September 2019; Accepted 25 September 2019

Available online 26 September 2019

1010-6030/ © 2019 Elsevier B.V. All rights reserved.



**Scheme 1.** The structure of molecular host **1** and reference molecule **2**.

many of the host-guest systems. Mechanical methods including solid state grinding and solvent assistant grinding could be used to prepare molecular co-crystals in simple and effective ways [27], and sometimes the resulting crystals are different from the ones from solution or melting crystallization path [28]. The interactions between the guest and the host are enhanced when the solvent is omitted [29].

Herein, we report a new type of fluorogenic material based on phenanthroimidazole moiety showing a mechanical and thermal response, as well as the response due to anion type and guest interactions. Phenanthroimidazole fluorophore has been used previously to design mechanoresponsive materials [30]. The molecular design of a host is essential for suitable guest-recognition by  $\pi$ - $\pi$  interaction to have a sensitive fluorescence response. For this purpose, we have designed and synthesized the molecular host **1** using fluorescent phenanthroimidazole pincers -with both  $\pi$ -donor and  $\pi$ -acceptor fragments- and benzylic spacer (Scheme 1). This dual nature of **1** causes the emission band to shift to longer wavelengths which are very important for biological applications and allows more effective interactions between host and different guests through  $\pi$ - $\pi$  interaction. Subsequently, we have studied the interactions between **1** as a host molecule with aromatic guests by grinding to form tunable color. Spectroscopy techniques were employed to investigate the effectiveness of grinding procedure to study the host-guest interactions and to compare it with the host-guest co-precipitates. The model compound **2** was synthesized as a reference for host-guest interaction, if any, to be compared with the molecular host **1**.

## 2. Experimental section

### 2.1. Materials and methods

All chemicals were purchased from Merck and used without further purification. All solvents were lab grade. The compounds **3** [31], **4** [32] and **5** [33] used in this study were synthesized according to the previously reported procedures.  $^1\text{H}$  NMR and  $^{13}\text{C}$  NMR spectra were recorded at room temperature by a Varian 500 MHz spectrometer. A Bruker TENSOR27 instrument measured FTIR-ATR spectra. Solution phase UV/Vis spectroscopy has been studied using a PerkinElmer Lambda 850 UV/Vis spectrophotometer. Diffuse Reflectance Spectra (DRS) were obtained using an Avantes Avaspec-2048-TEC spectrometer with AvaLamp DH-S setup using  $\text{BaSO}_4$  as the reflectance sample. Solid state and solution photoluminescence spectroscopy analyses were carried out by an Agilent G9800A fluorescence spectrophotometer. Solid sample holder with  $10 \times 10$  mm window used for powder compounds. The absolute solid-state fluorescence quantum yield measurements conducted on a Horiba Scientific Quanta- $\phi$  integrated sphere setup,

connected to a Fluoromax 4 fluorometer. Excitation performed at 380 nm. Powder X-ray Diffraction (PXRD) was collected on PANalytical X'PERT PRO MPD diffractometer using  $\text{CuK}\alpha$  irradiation. Scanning Electron Microscopy (SEM) micrographs obtained by a MIRA3, TESCAN instrument equipped with Energy Dispersive X-ray (EDX) and elemental mapping. Thermogravimetric Analysis (TGA) conducted on a TA Instruments Q50 Thermogravimetric System and samples were heated at a rate of  $20^\circ\text{C}/\text{min}$ . The balance and purge flows were 40 ml/min and 60 ml/min respectively. Electrostatic Potential Surface (EPS) calculations for guests were performed using SPARTAN 10 program. Optimization of geometry and Time-Dependent Density Functional Theory (TD-DFT) were performed using Gaussian 16 program. The structures were optimized initially by semi-empirical PM6 method and the optimized structures were used as input files for the DFT calculations at B3LYP/6-31 G(d) level of theory.

### 2.2. Synthesis of 1,1'-(2,5-bis(dodecyloxy)-1,4-phenylene)bis(methylene)bis(4-(1H-phenanthro[9,10-d]imidazol-2-yl)pyridinium) hexafluorophosphate (**1**)

A sealed tube was charged with 2,5-bis(bromomethyl)-1,4-bis(dodecyloxy)benzene (**4**) (0.5 mmol, 0.32 g), 2-(4-Pyridinyl)-1H-phenanthro [9,10-d]imidazole (**5**) (1.05 mmol, 0.31 g) and DMF (5 mL) and the mixture was heated to  $100^\circ\text{C}$  for 6 h. After cooling, the mixture was filtered off, washed with ethyl acetate and chloroform respectively, and dried at room temperature to afford yellow powder (yield: 70%). mp  $> 230^\circ\text{C}$ . ATR-FTIR ( $\text{cm}^{-1}$ )  $\nu$  3551-3296, 3039, 2935, 2847, 1635, 1421.  $^1\text{H}$ -NMR (500 MHz,  $\text{DMSO-d}_6$ )  $\delta$  9.30 (d,  $J = 6.5$  Hz, py-ring, 4 H), 9.06 – 8.94 (m, phenan-ring, 4 H), 8.89 (d,  $J = 4.5$  Hz, py-ring, 4 H), 8.56 – 8.42 (m, phenan-ring, 4 H), 7.91-7.81 (m, phenan-ring, 8 H), 7.57 (s, OR-phen-ring, 2 H), 5.91 (s, methylene, 4 H), 4.06 (s, O-methylene, 4 H), 1.70 (s,  $\text{CH}_2$ , 4 H), 1.28 – 0.81 (m,  $\text{CH}_2$ , 36 H), 0.77–0.70 (m,  $\text{CH}_3$ , 6 H).  $^{13}\text{C}$  NMR could not be obtained because of low solubility.

Ammonium hexafluorophosphate (0.8 mmol, 0.13 g) was added to the suspension of **1-Br** (0.3 mmol, 0.37 g) in methanol (30 mL). The mixture was stirred at room temperature for one hour. Then it was filtered off, washed with methanol and water respectively and dried at ambient temperature. Host **1** was obtained in quantitative yield as a yellow powder. mp  $> 230^\circ\text{C}$ .  $^1\text{H}$  NMR (500 MHz,  $\text{DMSO-d}_6$ )  $\delta$  9.27 (d,  $J = 6.3$  Hz, py-ring, 4 H), 9.00 (d,  $J = 8.5$  Hz, phenan-ring, 2 H), 8.97 (d,  $J = 8.5$  Hz, phenan-ring, 2 H), 8.87 (d,  $J = 6.3$  Hz, py-ring, 4 H), 8.51 (d,  $J = 8.0$  Hz, phenan-ring, 2 H), 8.45 (d,  $J = 8.5$  Hz, phenan-ring, 2 H), 7.86 (m, phenan-ring, 8 H), 7.55 (s, OR-phen-ring, 2 H), 5.89 (s, methylene, 4 H), 4.06 (t,  $J = 5.8$  Hz, O-methylene, 4 H), 1.70 (p,  $J = 7.3$  Hz,  $\text{CH}_2$ , 4 H), 1.21 (q,  $J = 7.3$  Hz,  $\text{CH}_2$ , 4 H), 1.17 – 0.99 (m,  $\text{CH}_2$ , 16 H), 0.95 – 0.79 (m,  $\text{CH}_2$ , 16 H), 0.73 (t,  $J = 7.3$  Hz,  $\text{CH}_3$ , 6 H).  $^{13}\text{C}$  NMR (126 MHz,  $\text{DMSO-d}_6$ )  $\delta$  156.30, 150.75, 146.28, 145.91, 139.92, 135.51, 129.96, 128.78, 128.61, 128.25, 128.17, 127.48, 124.54, 124.36, 124.19, 123.83, 123.74, 122.18, 121.32, 119.38, 116.19, 68.61, 60.09, 31.15, 29.32, 29.28, 29.13, 29.11, 28.93, 28.55, 28.48, 25.80, 21.98, 13.86. HRMS (ESI) calcd for  $\text{C}_{72}\text{H}_{82}\text{N}_6\text{O}_2^{2+}$  [ $\text{M}$ ] $^{2+}$ : 531.3244; found: 531.3266.

## 3. Results and discussion

### 3.1. Molecular design

Recently, in addition to  $^1\text{H}$ -NMR spectroscopy or single crystal formation, fluorescence spectrophotometry as an appropriate technique is used to study host-guest complexation because of easy detection and high sensitivity to low concentration of the complex [34]. Therefore, host **1** with fluorescent pincers and benzylic spacer was designed to study the interaction with aromatic guests. The pincer segment has a donor-acceptor characteristic causing strong CT from phenanthrene moiety to the pyridinium ring. The DFT method was used to optimize

the geometry and the optimized structure was utilized to calculate the electronic properties of host **1** by TD-DFT method at the level of B3LYP/6-31 G(d). The optimized structure of host **1** in global minimum conformation shows that the pincer fragments adopt a planar structure and anti positions around the spacer with a torsional angle of 160°. The highest occupied molecular orbital (HOMO) and the lowest unoccupied molecular orbital (LUMO) of host **1** are presented in Fig. S1 which shows that electron density distribution of HOMO is localized on the phenanthrene core, whereas LUMO is located mainly on pyridinium ring. The calculated results revealed the existence of the intramolecular charge transfer (ICT) process from phenanthrene as donor and pyridinium ring as acceptor through imidazole  $\pi$ -bridge in **1**. The large dipole moment in excited state (ES) compared to ground state (GS) is another evidence for the ICT. [35] The calculated dipole moment of host **1** in the GS and ES are 3.47 D and 14.08 D, respectively. The calculated  $\pi \rightarrow \pi^*$  transition (from the calculated UV-vis spectrum) is 1.54 eV which could be related to phenanthrene  $\pi$  orbitals (HOMO) to pyridinium ring  $\pi^*$  orbitals (LUMO). (Fig. S2)

### 3.2. Synthesis

The host **1** was prepared through the reaction between 2,5-bis(bromomethyl)-1,4-bis(dodecyloxy)benzene (**4**) and 2-(4-Pyridinyl)-1H-phenanthro [9,10-d]imidazole (**5**) in DMF at 100 °C to form 1-Br, and then the anion was exchanged by treating with ammonium hexafluorophosphate (Scheme 2). O-alkylation of hydroquinone formed compound **4** by 1-bromododecane in DMF followed by addition of methylene bromide using para-formaldehyde and hydrobromic acid in acetic acid. Simultaneously, compound **5** was synthesized from pyridine-4-carbaldehyde, 9,10-phenanthredione and an excess amount of ammonium acetate in acetic acid. Simple reactions, good yields, easy and inexpensive purifications (without usual chromatography procedures) are the advantages of synthetic procedure. Alkylation takes place at position 1 of the pyridine ring rather than imidazole. This expression is supported by the more significant changes in chemical shift of pyridine protons of compound **2** compared to compound **5** in the  $^1\text{H}$ NMR spectrum, i.e., a downfield shift of about 0.7 ppm for the ortho protons in pyridinium ring compared to the non-alkylated pyridine ring (Fig. S3). Hexafluorophosphate salt of **1** has been used for further investigation because the bromide salt is not emissive enough in the solid state. Unfortunately, despite all efforts, crystallization of host **1** was not successful, probably because of the existence of long alkyl chains.

### 3.3. Aggregation-induced emission enhancement (AIEE)

Host **1** is not soluble in most organic solvents. It only dissolves in a few polar solvents, in which, it did not show any solvato-chromic effects. The fluorescence analyses were performed in acetonitrile with

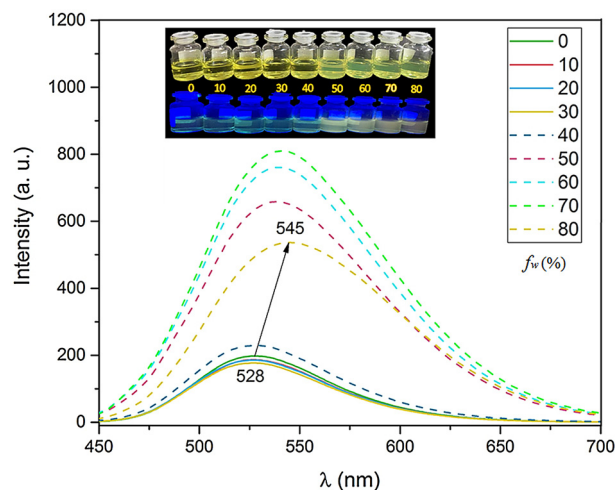
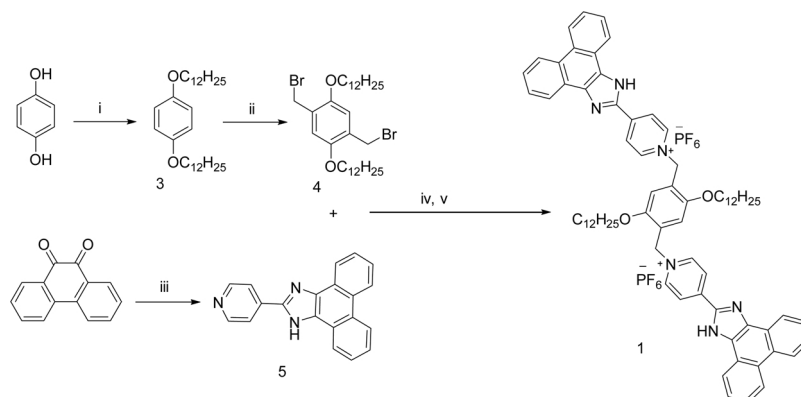


Fig. 1. Photographs (under daylight (top) and irradiation at 254 nm (down)) and emission spectra of host **1** in acetonitrile/water mixtures ( $\lambda_{\text{exc}} = 420 \text{ nm}$ ,  $c = 0.4 \mu\text{M}$ ) with different water fractions (fw).

different fractions of water to study the AIEE behavior of **1**. The solution of **1** in acetonitrile emits a greenish yellow light which does not change remarkably with increasing the water fraction up to 30%. Along with the formation of aggregates by addition of water from 40% to 70% as the solution turns cloudy, the PL intensity gradually increases and the emission shifts to yellow light (Fig. 1a). However, the PL intensity decreases when the water content reaches to 80% probably due to increase in the aggregate size or decrease in the crystallinity of particles. [36] At the same time the emission wavelength is shifted hypsochromically from 528 nm to 545 nm by increasing the solvent polarity by addition of water. These results imply that **1** could act as an AIEE active fluorescent molecule. Compared to host **1**, reference molecule **2** shows neither ACQ nor AIE effect with increasing water to THF ratio and no aggregation is observed in solution. (Fig. S4)

### 3.4. Mechano- and thermoresponsive behavior of **1**

The host **1** illustrates reversible mechanochromic and thermochromic behavior. The optical properties of host **1** before and after grinding was evaluated by diffuse-reflectance spectra (DRS) measurements (Fig. S5a). The host **1** shows a broad absorption peak between 250–500 nm. Grinding causes the absorption edge to shift to higher wavelengths (about 20 nm). This shift was observed as a change in color from yellow to orange by naked eyes. It has been found that the band gap is related to crystallinity [37] and particle size [38], mechanical grinding crashes the microcrystalline structure and might enforce



Scheme 2. Synthesis of molecular host **1**, i) 1-Bromododecane,  $\text{K}_2\text{CO}_3$ , DMF, reflux ii)  $\text{CH}_2\text{O}$ ,  $\text{HBr}/\text{CH}_3\text{COOH}$ , iii) Pyridine-4-carbaldehyde,  $\text{NH}_4\text{OAc}$ , acetic acid, iv) DMF, reflux, v)  $\text{NH}_4\text{PF}_6$ , acetone, r.t.

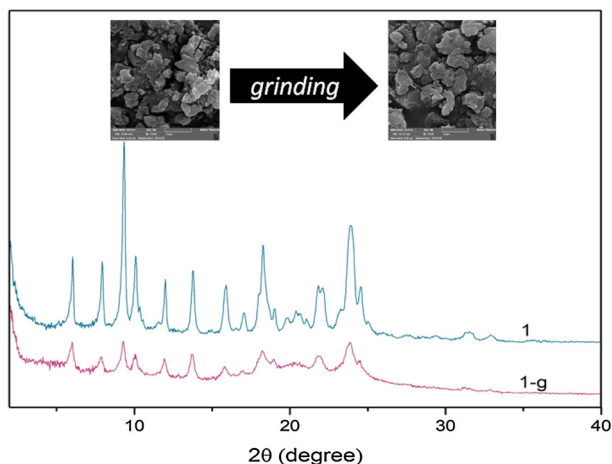


Fig. 2. PXRD patterns and SEM images of host 1 before and after grinding.

adhesion of small particles of the amorphous phase to each other leading to decrease the band gap from 2.30 eV for as-prepared host to 2.22 eV for the ground one (Fig. S5b). This issue was supported by SEM images and PXRD patterns as shown in Fig. 2. Before grinding, the host exhibits irregularly block-like aggregated microstructures with size less than 1  $\mu\text{m}$ . The mechanical grinding leads to a more amorphous and bulky structure. The broader and shorter signals for the ground compound compared to the sharp and intense signals of the host 1 in the PXRD patterns is a sign of the crashed microcrystalline structure and disordered molecular packing due to grinding. This comminuted particles sticks together to form an amorphous phase with larger particle size.

Moreover, the fluorescence emission changes from yellow ( $\lambda_{\text{max}} = 548 \text{ nm}$ ) to orange ( $\lambda_{\text{max}} = 556 \text{ nm}$ ) by grinding. On the other hand, the host 1 has a strong emission with an absolute quantum yield ( $\phi_f$ ) as much as 31% in the solid state and when it is ground, the absolute quantum yield decreases to 24%. Although the contrast is low between the two states but there are different methods to increase contrast in mechanochromic materials [39]. The optical properties of the ground compound returns to its initial state (as-prepared host) in contact with acetonitrile vapors (Fig. 3). It seems that the solvent molecules are able to reorganize damaged molecular packing. The very same effect has been reported in the literature [40]. According to thermogravimetric analysis (TGA), the excellent thermal stability of host 1 is indicated by

its high decomposition temperatures in the range of 255 – 280  $^{\circ}\text{C}$ . The TGA profile of host 1 reveals a 3% weight loss at around 90  $^{\circ}\text{C}$  probably due to the release of the trapped acetonitrile (Fig. S6). In addition, a change in color to deep-orange was observed in daylight when the as-prepared or ground powders were heated up to 120  $^{\circ}\text{C}$ , whereas the fluorescence intensity quenched utterly. After cooling to room temperature, the color turned immediately back to orange and the fluorescence emission intensity increased again. Interestingly,  $\lambda_{\text{max}}$  of emission of the cooled powder was observed to be identical to the  $\lambda_{\text{max}}$  of the ground compound, but not the original powder before heating ( $\lambda_{\text{max}} = 556 \text{ nm}$ ). With this findings in hand, we propose that grinding in addition to force sticking small aggregates to the bigger one, might also causes the release of the trapped solvent molecules resulting to color change [11a,41].

Also, the mechano and thermoresponsive behaviour were observed in reference molecule 2. Mechanical force shifts the emission peak to higher wavelength (about 30 nm). Similarly heating 2 causes too little color change although the spectrum of cooled powder was identical to initial sample. (Fig. S7)

### 3.5. Guest-responsive behavior

To consider the influence of different guests on the optical properties of host 1, first, the optical properties of host 1 and carbazole (CAB) as a guest was studied in the solution and then in the solid state. As shown in Fig. 4a, the absorbance spectrum of host 1 in acetonitrile shows notable broadband at 420 nm which could be attributed either to  $\pi-\pi^*$  transitions or formation of ICT between donor-acceptor moieties of the host itself. Addition of CAB as a guest to the solution did not have any distinctive effect on the absorption probably due to the weakness of  $\pi-\pi$  interactions compared with the interactions between the polar pincer and the solvent molecules, hindering the efficient interaction with guest. Also, for the solution of equimolar of host 1 and CAB, a weak CT band was observed at 650 nm. This result indicates that the CT complex was formed between host 1 and CAB. Likewise, a very little quenching of the broad emission band located at 527 nm in PL spectrum was observed via the addition of an equimolar amount of CAB to the solution of 1 (Fig. 4b).

For inclusion of guests into the host packing in the solid state, a mixture of pure materials was ground physically by agate mortar and pestle. A red shift occurred in the DRS spectrum of the ground mixture of 1 with CAB; comparing this spectrum with the one for the ground compound, the shift is more when the equivalent amount of CAB

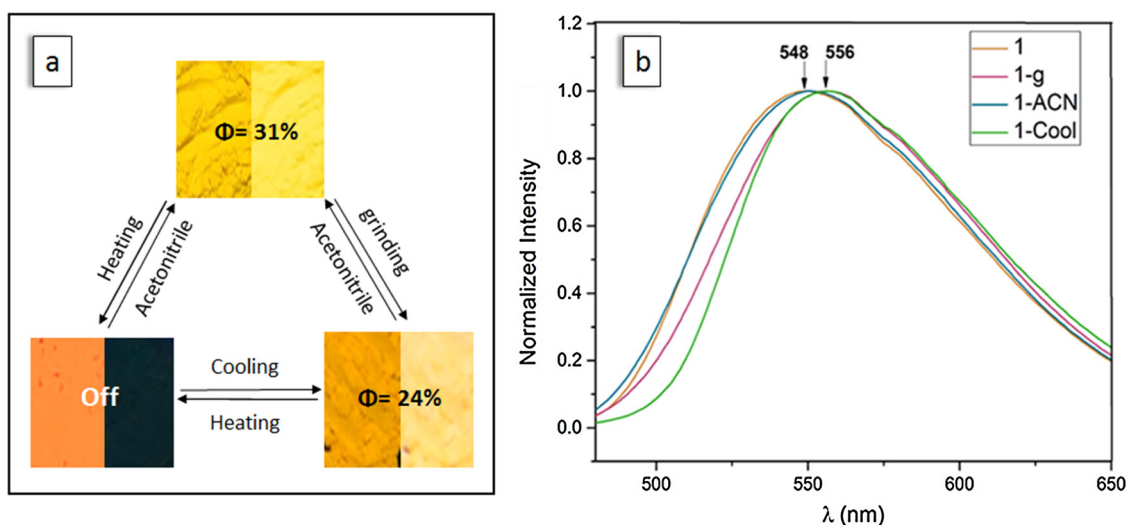


Fig. 3. a) Reversible diagram of host 1 photographs with different stimuli under UV light (irradiation at 254 nm) (right) and daylight (left); b) Emission spectra (excited at 330 nm) of host 1 under different stimuli.

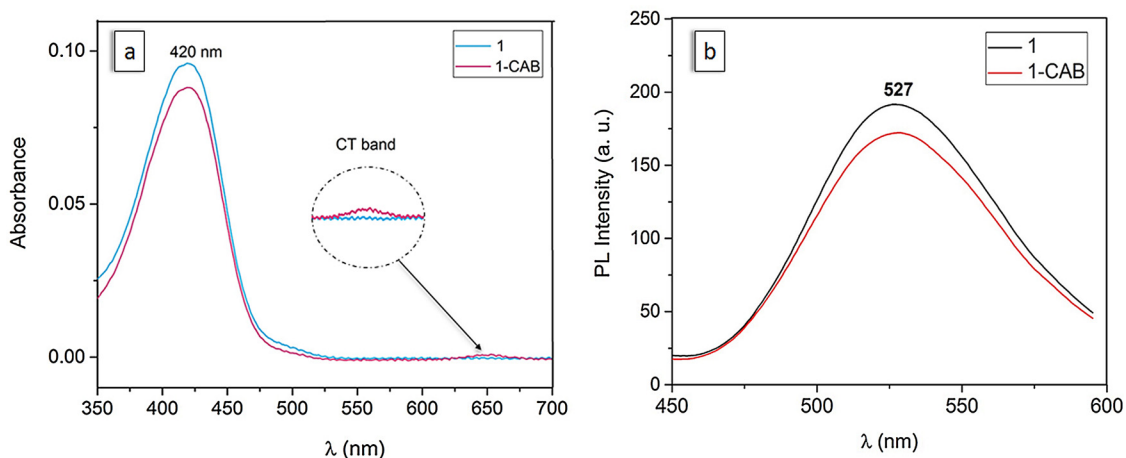


Fig. 4. a) The absorption spectra of host **1** in acetonitrile (2 μM) with a different equivalent of carbazole; b) The emission spectra (λ<sub>exc</sub>: 420 nm) of host **1** in acetonitrile (2 μM) in the presence of an equivalent of carbazole.

grounds with host **1**. The band gap also decreases more with the addition of CAB (Fig. S5). It should be noted from PXRD and SEM results that the crystallinity and particle size are almost the same for the ground host and the inclusion complex. Guest inclusion could reduce electronic band gap through CT in donor-acceptor systems which leads to an improved electrical conductivity [42]. The optical band gap of the **1** C CAB was calculated to be 2.15 eV.

During the grinding process, the color of the mixture gradually changed in day light, as well as under UV irradiation (Fig. 5a). The formation of CT complex as a consequence of grinding host **1** with

different series of electron-rich aromatic compounds developed a color range from army green to red-orange and caused significant fluorescence quenching. Because the host was dicationic, we chose electron-rich aromatic guests which expected to have maximum interaction. An extended π-π-stacking interaction seems to be the dominant interaction since some of these aromatic guests could not have any other type of intermolecular interactions. The broad emission band of host **1** at 556 nm shifted within 40 nm (in the range of 542–582 nm) with different guests such as 1,5-naphthalene diol (NDO), phenanthrene (Phen), anthracene (AN), pyrene (Py), 1,4-phenylene diamine (PDA),

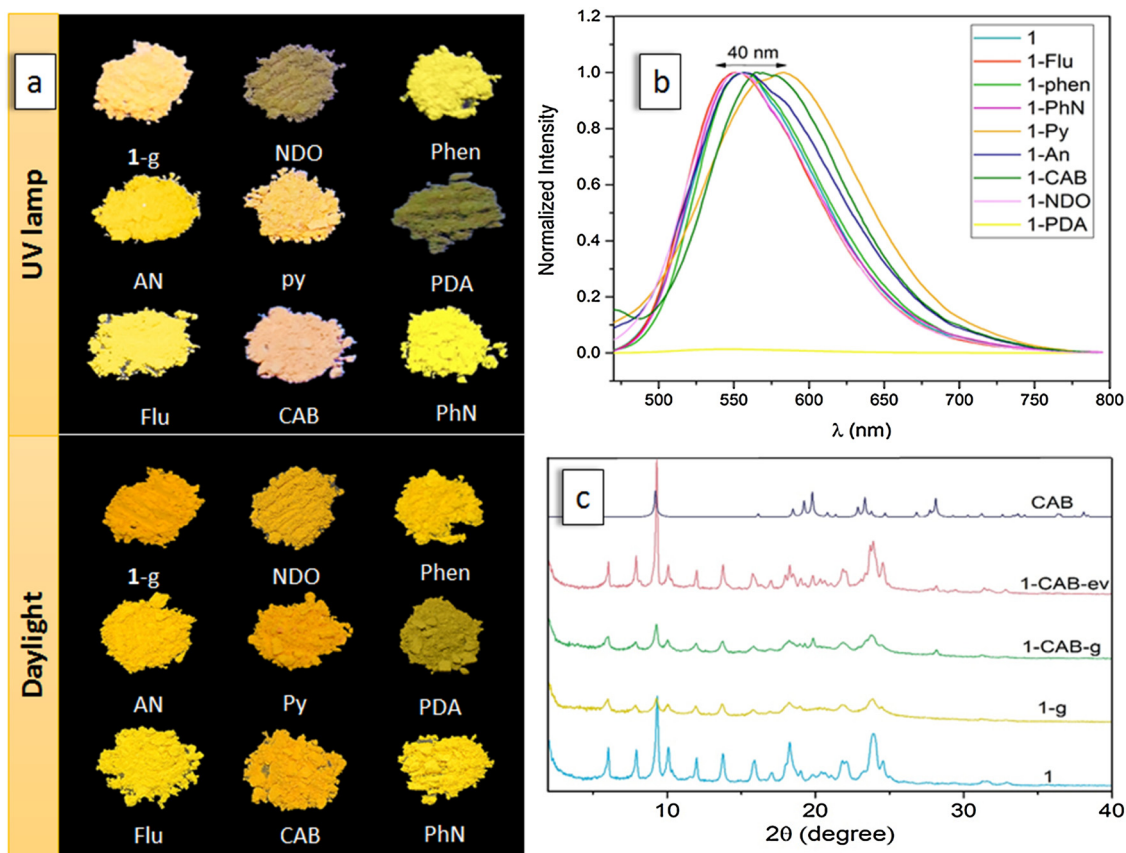


Fig. 5. a) Photographs of host **1** and its complex with guest under daylight and UV lamp (irradiation at 254 nm); b) The solid state emission spectra (excited at 330 nm) of host **1** with different guests (1:1); c) PXRD pattern of host **1** as-prepared (cyan line), **1** in the ground state (yellow line), **1** ground with carbazole (green line), **1** and carbazole co-precipitated (pink line) and theoretical powder pattern from a CIF of carbazole crystal (blue line).

fluoren-9-one (Flu), carbazole (CAB) and phenanthroline (PhN) (Fig. 5b). None of the guests have emission band in the range of 500–700 nm [43]. Therefore, they should have no contribution in the observed fluorescence emission. Engineering the effective interactions and prediction of  $\pi$ -donor strengths of guest molecules have been described previously by employing the calculated molecular electrostatic potential surface and Hammett substituent constants [44]. We used electrostatic potential maps to align guest interaction trends in order to interpret the acquired results in this study (Fig. S8). The calculations were carried out by DFT method using B3LYP/6-31 G(d) level of theory. PDA and NDO showed the most quench in PL diagram. PDA is completely quenched but the absolute quantum yield for NDO is 1.8%. According to calculated electrostatic potential maps, these guest molecules provide high electron density surfaces and are expected to show the most efficient interactions with the electron-deficient host **1**. Py, PhN, Phen and CAB are known to be suitable electron donors, showing more quenching effect compared with fluoren-9-one and anthracene. The absolute quantum yield for **1**  $\subset$  Py, CAB, PhN and Phen complexes are 4.6, 4.8, 4.9 and 5.1% respectively, which are about five times lower than the ground form. The absolute quantum yield for Flu and An are 14 and 8.1% respectively, due to weak interaction with host **1**. Furthermore, Py and CAB illustrate bathochromic (red) shift. These results indicate the strong CT interaction between host and guest that leads to quenching and red shift in the spectrum.

Besides, SEM-EDX elemental mapping was used to confirm if the inclusion occurs uniformly during the grinding of host **1**/guest or only a physical mixture is formed. For this purpose, the mixture of host **1** and 3,6-dibromocarbazole as a guest, grounded together and elemental distribution was studied. The Br atom merely was presented in the guest molecule while P and F atoms existed just in the host molecule. Fig. S9, shows that all of the elements (C, O, Br, P, and F) are distributed homogeneously, indicating that grinding was able to put the host and the guest uniformly together. Also, it can be concluded from the homogeneity that the product is an inclusion compound rather than a physically mixture. Because, obtaining a completely homogenous blends from physically mixing microcrystalline structures is a very rare case.

The difference between the grinding procedure and co-precipitation to form inclusion compounds was studied by co-precipitation of CAB and the host **1** from the acetonitrile-chloroform mixture through solvent evaporation. Then, the PL spectrum of this micro-crystalline powder compared with the ground one; grinding of **1** with CAB ( $\varphi_f = 4.8\%$ ) shows more quenching effect than co-precipitation procedure ( $\varphi_f = 8.9\%$ ) (Fig. 6a). The crystalline-induced emission enhancement

(CIEE) effect [45] was observed in sample which was produced by co-precipitation method which is supported by PXRD results. Also, the red shift in co-precipitation method ( $\lambda_{\max} = 579$  nm) is more than grinding one ( $\lambda_{\max} = 567$  nm). Because the molecules in the solution have more chance to make suitable arrangement for effective interactions. In the PXRD pattern of the co-precipitated complex, new peaks appeared while the crystalline structure of the host preserved. The similarity of this pattern with the one from pure host **1** as-prepared, could be used as evidence to prove that the observed red shift is due to the interaction of **1** with CAB. The new peaks are similar to CAB pattern obtained from its CIF file. The peaks in the PXRD pattern of the co-precipitation procedure are sharp while in the ground material presence of more amorphous phase causes peak broadening.

There remains a question, whether the structure of host **1** is necessary to interact with guests or the pincer alone could be enough? To answer this question and to have more insight about guest-responsive behavior, compound **2**, as a reference molecule, has been synthesized and its interaction with CAB as a guest was compared with the host **1**. As can be seen from Fig. 6b, the ground mixture of CAB with compound **2** does not show any difference with the ground pure **2**. In conclusion, the whole structure of **1** is responsible for the observed phenomena.

#### 4. Counterion responsive behavior

Organic salts play an important role in construction of supramolecular assemblies [46] and the arrangement in self-assembled structures could be simply modified by changing the counter ion [47]. Moreover, the ionic materials are often conductive and therefore can find potential applications in solar cells or photovoltaic devices [48] and some of them have also been used in imaging [49]. The electrostatic attraction between the cationic chromophore and anionic moiety could be used to tune the luminescence properties of the emissive compounds [50]. It is proved that anion exchange can affect the emission because of the coulombic attraction and steric effects which appear in molecular packing of crystals or aggregates [51]. The effect of counterion on light emission was studied by measuring the fluorescence spectra of host **1** with different anions. The absolute quantum yield and the  $\lambda_{\max}$  changes drastically when anion exchange takes place. The amount of quantum yield for  $F^-$ ,  $SCN^-$  and  $Br^-$  anions are low (about 1.54, 1.26 and 0.88% respectively) while  $I^-$  and  $B(Ph)_4^-$  anions/host **1** are not emissive. However,  $PF_6^-$ ,  $ClO_4^-$  and  $Cl^-$  anions/host **1** are highly emissive and quantum yield are 31.5, 11.9 and 7.2% respectively. The shift due to anion exchange occurs in the range of 522–578 nm (Fig. 7). Tetraphenylborate is a very big anion. Thus, the steric repulsion between the

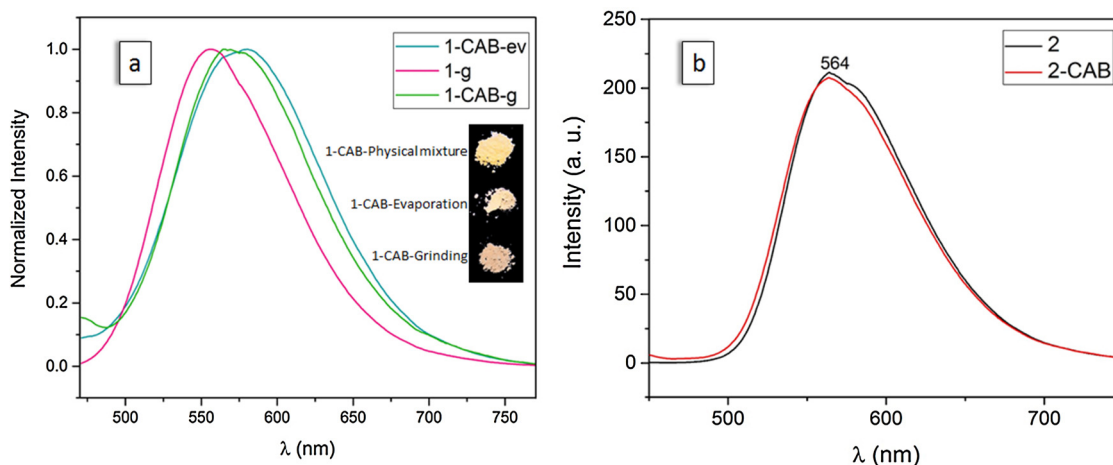


Fig. 6. a) The solid state PL spectra of compound **1** and its carbazole complex prepared by grinding and evaporation procedure (excited at 330 nm) and photograph (under irradiation at 254 nm) of host **1**-carbazole with different method preparation; b) The solid state emission spectra of compound **2** and its grinding mixture with carbazole (1:1).

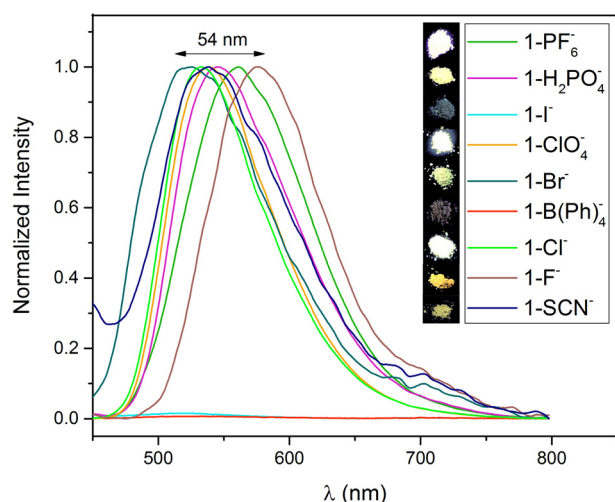


Fig. 7. The normalized solid state emission spectra (excited at 330 nm) and photographs (under irradiation at 254 nm) of host 1 and different counterions.

anion and host 1 probably affects molecular planarity and packing of host 1 [50a].  $F^-$  is a small anion which might cause close packing of aromatic sheets, as a consequence 1- $F^-$  is less emissive than 1- $PF_6^-$ . The heavy atom effect due to increased non-radiative relaxation leads to quenching when iodide and bromide anions are the counter ion of host 1 [52]. A red shift was observed in the case of  $PF_6^-$  anion suggesting the possibility of J-aggregate formation. These results suggest that the emission not only is affected by the anion size but also the affinity between the cation and anion moiety.

Reference molecule 2 with different anions have been prepared by the same procedures of 1 and counter anions. Measuring PL spectra of these compounds show that molecule 2 is also capable of distinguishing between different anions but there are differences between the responses of the two molecules (1 & 2), the reason of that is under study. (Fig. S10)

## 5. Conclusions

In summary, the molecular host 1 with multi-stimuli responsive behavior designed, synthesized and its properties studied. This host shows piezochromic behavior, as mechanical force can alter the PL peak position to longer wavelengths within 8 nm, returning to its initial state after contact with acetonitrile vapors. Also, when host 1 heated to 120 °C, the color changed to deep orange and its fluorescence quenched, but it turned back to the initial color after cooling down to room temperature. The host-guest complexation studied in the solid state via mechanical grinding. Different guests shift the PL spectrum in a range of 40 nm, leading to tunable color. The formation of charge transfer complex between host and guest is able to significantly decrease absolute quantum yield. Moreover, the DRS measurements indicated that the addition of guests can decrease the band gap energy. UV-vis spectroscopy and PXRD analysis were used to study the CAB inclusion through grinding and co-precipitation. The SEM-EDX elemental measurements confirmed that a very homogeneous entity of host 1/guest is formed. The counterion role in the PL properties studied by anion exchange suggests that the emission is affected by the anion size and the affinity between cation and anion moiety.

## Declaration of Competing Interest

There is no competing interest to declare.

## Acknowledgements

The financial support by the Research Council of the University of Tehran is acknowledged. The authors are grateful to Ehsan Hamzepour for useful help with DFT calculations.

## Appendix A. Supplementary data

Supplementary material related to this article can be found, in the online version, at doi:<https://doi.org/10.1016/j.jphotochem.2019.112106>.

## References

- [1] (a) C. Weder, C. Sarwa, A. Montali, C. Bastiaansen, P. Smith, Incorporation of photoluminescent polarizers into liquid crystal displays, *Science* 279 (1998) 835–837; (b) S. Hirata, T. Watanabe, Reversible thermoresponsive recording of fluorescent images (TRF), *Adv Mater* 18 (2006) 2725–2729; (c) S.C. Mannsfeld, B.C. Tee, R.M. Stoltenberg, C.V. Chen, S. Barman, B.V. Muir, A.N. Sokolov, C. Reese, Z. Bao, Highly sensitive flexible pressure sensors with microstructured rubber dielectric layers, *Nat. Mater.* 9 (2010) 859–864; (d) L. Pan, A. Chortos, G. Yu, Y. Wang, S. Isaacson, R. Allen, Y. Shi, R. Dauskardt, Z. Bao, An ultra-sensitive resistive pressure sensor based on hollow-sphere microstructure induced elasticity in conducting polymer film, *Nat. Commun.* 5 (2014) 3002.
- [2] (a) S. Durben, T. Baumgartner, 3,7-Diazadibenzophosphine oxide: a phosphorus-bridged viologen analogue with significantly lowered reduction threshold, *Angew. Chem. Int. Ed.* 50 (2011) 7948–7952; (b) M. Stolar, J. Borau-Garcia, M. Toonen, T. Baumgartner, Synthesis and tunability of highly electron-accepting, N-benzylated “Phosphaviologens”, *J. Am. Chem. Soc.* 137 (2015) 3366–3371.
- [3] (a) J.W. Chung, Y. You, H.S. Huh, B.K. An, S.J. Yoon, S.H. Kim, S.W. Lee, S.Y. Park, Shear- and UV-induced fluorescence switching in stilbene  $\pi$ -dimer crystals powered by reversible [2 + 2] cycloaddition, *J. Am. Chem. Soc.* 131 (2009) 8163–8172; (b) D. Kim, S.Y. Park, Multicolor fluorescence photoswitching: color-correlated versus color-specific switching, *Adv. Opt. Mater.* 6 (2018) 1800678.
- [4] (a) Y. Hong, Aggregation-induced emission-fluorophores and applications, *Methods Appl. Fluoresc.* 4 (2016) 022003; (b) Y. Dong, B. Xu, J. Zhang, X. Tan, L. Wang, J. Chen, H. Lv, S. Wen, B. Li, L. Ye, B. Zou, W. Tian, Piezochromic luminescence based on the molecular aggregation of 9,10-bis((E)-2-(pyrid-2-yl)vinyl)anthracene, *Angew. Chem. Int. Ed.* 51 (2012) 10782–10785; (c) Y. Hong, J.W.Y. Lam, B.Z. Tang, Aggregation-induced emission: phenomenon, mechanism and applications, *Chem. Commun. (Camb.)* 0 (2009) 4332–4353.
- [5] (a) C. Reichardt, Solvatochromic dyes as solvent polarity indicators, *Chem. Rev.* 94 (1994) 2319–2358; (b) P. Wen, Z. Gao, R. Zhang, A. Li, F. Zhang, J. Li, J. Xie, Y. Wu, M. Wu, K.P. Guo, A- $\pi$ -D- $\pi$ -A carbazole derivatives with remarkable solvatochromism and mechanoresponsive luminescence turn-on, *J. Mater. Chem. C Mater. Opt. Electron. Devices* 5 (2017) 6136–6143; (c) J. Lee, H.T. Chang, H. An, S. Ahn, J. Shim, J.M. Kim, A protective layer approach to solvatochromic sensors, *Nat. Commun.* 4 (2013) 2461.
- [6] (a) A. Seeboth, J. Kriwanek, R. Vetter, The first example of thermochromism of dyes embedded in transparent polymer gel networks, *J. Mater. Chem.* 9 (1999) 2277–2278; (b) S.J. Osborne, S. Wellens, C. Ward, S. Felton, R.M. Bowman, K. Binnemans, M. Swadźba-Kwaśny, H.Q.N. Gunaratne, P. Nockemann, Thermochromism and switchable paramagnetism of cobalt (II) in thiocyanate ionic liquids, *Dalton Trans.* 44 (2015) 11286–11289.
- [7] (a) Y. Sagara, T. Komatsu, T. Ueno, K. Hanaoka, T. Kato, T. Nagano, A water-soluble mechanochromic luminescent pyrene derivative exhibiting recovery of the initial photoluminescence color in a high-humidity environment, *Adv. Funct. Mater.* 23 (2013) 5277–5284; (b) Y. Sagara, S. Yamane, M. Mitani, C. Weder, T. Kato, Mechanoresponsive luminescent molecular assemblies: an emerging class of materials, *Adv. Mater.* 28 (2016) 1073–1095; (c) Y. Sagara, C. Weder, N. Tamaoki, Tuning the thermo- and mechanoresponsive behavior of luminescent cyclophanes, *RSC Adv.* 6 (2016) 80408–80414.
- [8] (a) M.S. Moorthy, S. Bharathiraja, P. Manivagan, K.D. Lee, J. Oh, Synthesis of surface capped mesoporous silica nanoparticles for pH-stimuli responsive drug delivery applications, *Med. Chem. Res.* 8 (2017) 1797–1800; (b) X. Yao, X. Ma, H. Tian, Aggregation-induced emission encoding supramolecular polymers based on controllable sulfonatocalixarene recognition in aqueous solution, *J. Mater. Chem. C Mater. Opt. Electron. Devices* 2 (2014) 5155–5160; (c) G. Kocak, C. Tuncer, V. Büttin, pH-Responsive polymers, *Polym. Chem.* 8 (2017) 144–176.
- [9] (a) M. Yamaguchi, S. Ito, A. Hirose, K. Tanaka, Y. Chujo, Control of aggregation-induced emission versus fluorescence aggregation-caused quenching by bond existence at a single site in boron pyridinoiminate complexes, *Mater. Chem. Front.* 1 (2017) 1573–1579;

- (b) Z. Chen, D. Wu, X. Han, Y. Nie, J. Yin, G.A. Yu, S.H. Liu, 1,8-Naphthalimide-based highly blue-emissive fluorophore induced by a bromine atom: reversible thermochromism and vapochromism characteristics, *RSC Adv.* 4 (2014) 63985–63988.
- [10] (a) H. Ito, T. Saito, N. Oshima, N. Kitamura, S. Ishizaka, Y. Hinatsu, M. Wakeshima, M. Kato, K. Tsuge, M. Sawamura, Reversible mechanochromic luminescence of [(C6F5Au)<sub>2</sub>(μ-1,4-diisocyanobenzene)], *J. Am. Chem. Soc.* 130 (2008) 10044–10045; (b) M.S. Kwon, J. Gierschner, S.J. Yoon, S.Y. Park, Unique piezochromic fluorescence behavior of dicyanodistyrylbenzene based donor-acceptor-donor triad: mechanically controlled photo-induced electron transfer (eT) in molecular assemblies, *Adv. Mater.* 24 (2012) 5487–5492; (c) J. Luo, L.Y. Li, Y. Song, J. Pei, A piezochromic luminescent complex: mechanical force induced patterning with a high contrast ratio, *Chem. Eur. J.* 17 (2011) 10515–10519.
- [11] (a) T. Seki, T. Ozaki, T. Okura, K. Asakura, A. Sakon, H. Uekusa, H. Ito, Interconvertible multiple photoluminescence color of a gold(I) isocyanide complex in the solid state: solvent-induced blue-shifted and mechano-responsive red-shifted photoluminescence, *Chem. Sci.* 6 (2015) 2187–2195; (b) C. Dou, L. Han, S. Zhao, H. Zhang, Y. Wang, Multi-stimuli-responsive fluorescence switching of a donor-acceptor π-conjugated compound, *J. Phys. Chem. Lett.* 2 (2011) 666–670; (c) Y. Sagara, T. Kato, Brightly tricolored mechanochromic luminescence from a single-luminophore liquid crystal: reversible writing and erasing of images, *Angew. Chem. Int. Ed.* 50 (2011) 9128–9132.
- [12] (a) Y. Zhang, K. Wang, G. Zhuang, Z. Xie, C. Zhang, F. Cao, G. Pan, H. Chen, B. Zou, Y. Ma, Multicolored-fluorescence switching of ICT-type organic solids with clear color difference: mechanically controlled excited state, *Chem. Eur. J.* 21 (2015) 2474–2479; (b) Y.J. Pu, M. Higashidate, K. Nakayama, J. Kido, Solution-processable organic fluorescent dyes for multicolor emission in organic light emitting diodes, *J. Mater. Chem.* 18 (2008) 4183–4188.
- [13] X. Wang, Y. Xu, X. Ma, H. Tian, Multicolor photoluminescence of a hybrid film via the dual-emitting strategy of an inorganic fluorescent Au nanocluster and an organic room-temperature phosphorescent copolymer, *Ind. Eng. Chem. Res.* 57 (2018) 2866–2872.
- [14] (a) M.S. Wang, S.P. Guo, Y. Li, L.Z. Cai, J.P. Zou, G. Xu, W.W. Zhou, F.K. Zheng, G.C. Guo, A direct white-light-emitting metal-organic framework with tunable yellow-to-white photoluminescence by variation of excitation light, *J. Am. Chem. Soc.* 131 (2009) 13572–13573; (b) R.J. Marshall, Y. Kalinovsky, S.L. Griffin, C. Wilson, B.A. Blight, R.S. Forgan, Functional versatility of a series of Zr metal-organic frameworks probed by solid-state photoluminescence spectroscopy, *J. Am. Chem. Soc.* 139 (2017) 6253–6260.
- [15] D. Zhou, D. Li, P. Jing, Y. Zhai, D. Shen, S. Qu, A.L. Rogach, Conquering aggregation-induced solid-state luminescence quenching of carbon dots through a carbon dots-triggered silica gelation process, *Chem. Mater.* 29 (2017) 1779–1787.
- [16] F. Zhang, R. Zhang, X. Liang, K. Guo, Z. Han, X. Lu, J. Xie, J. Li, D. Li, X. Tian, 1,3-Indanedione functionalized fluorene luminophores: negative solvatochromism, nanostructure-morphology determined AIE and mechanoresponsive luminescence turn-on, *Dyes Pigm.* 155 (2018) 225–232.
- [17] (a) Y. Matsunaga, J.S. Yang, Multicolor fluorescence writing based on host-guest interactions and force-induced fluorescence-color memory, *Angew. Chem. Int. Ed.* 54 (2015) 7985–7989; (b) M. Zhang, S. Yin, J. Zhang, Z. Zhou, M.L. Saha, C. Lu, P.J. Stang, Metallacyclic supramolecular assemblies with tunable fluorescence including white-light emission, *Proc. Natl. Acad. Sci. U. S. A.* 114 (2017) 3044–3049; (c) D. Yan, Y. Tang, H. Lin, D. Wang, Tunable two-color luminescence and host-guest energy transfer of fluorescent chromophores encapsulated in metal-organic frameworks, *Sci. Rep.* 4 (4337) (2014); (d) D. Yan, J. Lu, J. Ma, S. Qin, M. Wei, D.G. Evans, X. Duan, Layered host-guest materials with reversible piezochromic luminescence, *Angew. Chem. Int. Ed.* 50 (2011) 7037–7040.
- [18] (a) L. Yang, Y. Ding, Y. Yang, Y. Yan, J. Huang, A.D. Keizer, M.A.C. Stuart, Fluorescence enhancement by microphase separation-induced chain extension of Eu<sup>3+</sup> coordination polymers: phenomenon and analysis, *Soft Matter* 7 (2011) 2720–2724; (b) A.O. Weldeab, A. Steen, D.J. Starkenburg, J.S.D. Williams, K.A. Abboud, J. Xue, N.I. Hammer, R.K. Castellano, D.L. Watkins, Tuning the structural and spectroscopic properties of donor-acceptor-donor oligomers via mutual X-bonding, H-bonding, and π-π interactions, *J. Mater. Chem. C Mater. Opt. Electron. Devices* 6 (2018) 11992–12000; (c) A. Wang, R. Fan, Y. Dong, W. Chen, Y. Song, P. Wang, S. Hao, Z. Liu, Y. Yang, (E)-4-Methyl-N-((quinolin-2-yl)ethylidene)aniline as ligand for IIB supramolecular complexes: synthesis, structure, aggregation-induced emission enhancement and application in PMMA-doped hybrid material, *Dalton Trans.* 46 (2017) 71–85.
- [19] (a) L.M. Salonen, M. Ellermann, F. Diederich, Aromatic rings in chemical and biological recognition: energetics and structures, *Angew. Chem. Int. Ed.* 50 (2011) 4808–4842; (b) E.M. Pérez, N. Martín, π-π interactions in carbon nanostructures, *Chem. Soc. Rev.* 44 (2015) 6425–6433; (c) M. Paulino, G. Grisci, G. Giuliani, I. Zanardi, M. Andreassi, V. Travagli, M. Licciardi, C. Scialabba, G. Giammona, A. Cappelli, S. Vomero, π-Stacked polymers in drug delivery applications, *J. Drug Deliv. Sci. Technol.* 32 (2016) 142–166.
- [20] (a) G. Zhang, Q. Chen, Y. Zhang, L. Kong, X. Tao, H. Lu, Y. Tian, J. Yang, Bulky group functionalized porphyrin and its Zn(II) complex with high emission in aggregation, *Inorg. Chem. Commun.* 46 (2014) 85–88; (b) Y. Sun, Q. Huang, X. Zhang, X. Ding, P. Han, B. Lin, H. Yang, L. Guo, Functionalization of side chain terminals with fused aromatic rings in carbazole-diketopyrrolopyrrole based conjugated polymers for improved charge transport properties, *RSC Adv.* 6 (2016) 97783–97790.
- [21] (a) Y. Shao, G.Z. Yin, X. Ren, X. Zhang, J. Wang, K. Guo, X. Li, C. Wesdemiotis, W.B. Zhang, S. Yang, M. Zhu, B. Sun, Engineering π-π interactions for enhanced photoluminescent properties: unique discrete dimeric packing of perylene diimides, *RSC Adv.* 7 (2017) 6530–6537; (b) J.S. Yang, J.L. Yan, Central-ring functionalization and application of the rigid, aromatic, and H-shaped pentyptycene scaffold, *Chem. Commun. (Camb.)* 0 (2008) 1501–1512; (c) J.S. Yang, T.M. Swager, Porous shape persistent fluorescent polymer films: an approach to TNT sensory materials, *J. Am. Chem. Soc.* 120 (1998) 5321–5322.
- [22] Y.T. Lee, C.L. Chiang, C.T. Chen, Solid-state highly fluorescent diphenylaminospirofluorenylfumarone nitrile red emitters for non-doped organic light-emitting diodes, *Chem. Commun. (Camb.)* 0 (2008) 217–219.
- [23] (a) S. Hecht, J.M.J. Frechet, Dendritic encapsulation of function: applying nature's site isolation principle from biomimetics to materials science, *Angew. Chem. Int. Ed.* 40 (2001) 74–91; (b) C.W. Wu, C.M. Tsai, H.C. Lin, Synthesis and characterization of poly(fluorene)-based copolymers containing various 1,3,4-oxadiazole dendritic pendants, *Macromolecules* 39 (2006) 4298–4305.
- [24] (a) J. Luo, Z. Xie, J.W.Y. Lam, L. Cheng, H. Chen, C. Qiu, H.S. Kwok, X. Zhan, Y. Liu, D. Zhu, B.Z. Tang, Aggregation-induced emission of 1-methyl-1,2,3,4,5-pentaphenylsilole, *Chem. Commun. (Camb.)* 0 (2001) 1740–1741; (b) B.K. An, S.K. Kwon, S.D. Jung, S.Y. Park, Enhanced emission and its switching in fluorescent organic nanoparticles, *J. Am. Chem. Soc.* 124 (2002) 14410–14415.
- [25] (a) Q. Zhang, D.H. Qu, X. Ma, H. Tian, Sol-gel conversion based on photoswitching between noncovalently and covalently linked netlike supramolecular polymers, *Chem. Commun. (Camb.)* 49 (2013) 9800–9802; (b) Q. Zhang, D.H. Qu, J. Wu, X. Ma, Q. Wang, H. Tian, A Dual-modality photo-switchable supramolecular polymer, *Langmuir* 29 (2013) 5345–5350; (c) R. Sun, C. Xue, X. Ma, M. Gao, H. Tian, Q. Li, Light-driven linear helical supramolecular polymer formed by molecular-recognition-directed self-assembly of bis(p-sulfonatocalix[4]arene) and pseudorotaxane, *J. Am. Chem. Soc.* 135 (2013) 5990–5993; (d) Q. Zhang, X. Yao, D.H. Qu, X. Ma, Multistate self-assembled micro-morphology transitions controlled by host-guest interactions, *Chem. Commun. (Camb.)* 50 (2014) 1567–1569.
- [26] (a) Q.W. Zhang, D. Li, X. Li, P.B. White, J. Mecinović, X. Ma, H. Ågren, R.J.M. Nolte, H. Tian, Multicolor photoluminescence including white-light emission by a single host-guest complex, *J. Am. Chem. Soc.* 138 (2016) 13541–13550; (b) J. Sun, L. Shao, J. Zhou, B. Hua, Z. Zhang, Q. Li, J. Yang, Efficient enhancement of fluorescence emission via TPE functionalized cationic pillar[5]arene-based host-guest recognition-mediated supramolecular self-assembly, *Tetrahedron Lett.* 59 (2018) 147–150; (c) J. Sun, B. Hua, Q. Li, J. Zhou, J. Yang, Acid/Base-controllable FRET and self-assembling systems fabricated by rhodamine B functionalized pillar[5]arene-based host-guest recognition motifs, *Org. Lett.* 20 (2018) 365–368; (d) D. Wu, Y. Li, J. Yang, J. Shen, J. Zhou, Q. Hu, G. Yu, G. Tang, X. Chen, Supramolecular nanomedicine constructed from cucurbit[8]uril-based amphiphilic brush copolymer for Cancer therapy, *ACS Appl. Mater. Interfaces* 9 (2017) 44392–44401.
- [27] (a) K.T. Holman, A.M. Pivovar, M.D. Ward, Engineering crystal symmetry and polar order in molecular host frameworks, *Science* 294 (2001) 1907–1911; (b) T. Friscic, A.V. Trask, W. Jones, W.D.S. Motherwell, Screening for inclusion compounds and systematic construction of three-component solids by liquid-assisted grinding, *Angew. Chem. Int. Ed.* 45 (2006) 7546–7550; (c) Y.M. Wang, Z.Y. Wu, H.J. Wang, J.H. Zhu, Fabrication of metal oxides occluded in ordered mesoporous hosts via a solid-state grinding route: the influence of host-guest interactions, *Adv. Funct. Mater.* 16 (2006) 2374–2386; (d) R. Giustetto, J.G. Vitillo, I. Corazzari, F. Turci, Evolution and reversibility of host/guest interactions with temperature changes in a methyl red/palygorskite polyfunctional hybrid nanocomposite, *J. Phys. Chem. C* 118 (2014) 19322–19337.
- [28] E.Y. Cheung, S.J. Kitchin, K.D.M. Harris, Y. Imai, N. Tajima, R. Kuroda, Direct structure determination of a multicomponent molecular crystal prepared by a solid-state grinding procedure, *J. Am. Chem. Soc.* 125 (2003) 14658–14659.
- [29] (a) H. Sohn, M.J. Sailor, D. Magde, W.C. Troglor, Detection of nitroaromatic explosives based on photoluminescent polymers containing metalloles, *J. Am. Chem. Soc.* 125 (2003) 3821–3830; (b) D. Zhao, T.M. Swager, Sensory responses in solution vs solid state: a fluorescence quenching study of poly(ptycenebutadiynylene)s, *Macromolecules* 38 (2005) 9377–9384.
- [30] (a) G. Li, J. Zhao, D. Zhang, Z. Shi, Z. Zhu, H. Song, J. Zhu, S. Tao, F. Lu, Q. Tong, Mechanochromic asymmetric sulfone derivatives for use in efficient blue organic light-emitting diodes, *J. Mater. Chem. C Mater. Opt. Electron. Devices* 4 (2016) 8787–8794; (b) A. Ekbote, S.H. Han, T. Jadhav, S.M. Mobin, J.Y. Lee, R. Misra, Stimuli responsive AIE active positional isomers of phenanthroimidazole as non-doped emitters in OLEDs, *J. Mater. Chem. C Mater. Opt. Electron. Devices* 6 (2018) 2077–2087; (c) Z.Y. Wang, J.W. Zhao, P. Li, T. Feng, W.J. Wang, S.L. Tao, Q.X. Tong, Novel phenanthroimidazole-based blue AIEgens: reversible mechanochromism, bipolar transporting properties, and electroluminescence, *New J. Chem.* 42 (2018) 8924–8932.
- [31] A. Llanes-Pallas, K. Yoosaf, H. Traoulsi, J. Mohanraj, T. Seldrum, J. Dumont,

- A. Minoia, R. Lazzaroni, N. Armaroli, D. Bonifazi, Modular engineering of H-bonded supramolecular polymers for reversible functionalization of carbon nanotubes, *J. Am. Chem. Soc.* 133 (2011) 15412–15424.
- [32] B. Wang, M.R. Wasielewski, Design and synthesis of metal ion-recognition-induced conjugated polymers: an approach to metal ion sensory materials, *J. Am. Chem. Soc.* 119 (1997) 12–21.
- [33] L. Achremowicz, M. Jastrzebska-Glapa, K. Kloc, J. Mlochowski, Investigations on reactivity of phenanthrolines. Part IX. Extension of 1,7- and 1,8-phenanthroline systems by azaaromatic rings, *Pol. J. Chem.* 54 (1980) 2365–2372.
- [34] R.N. Dsouza, U. Pischel, W.M. Nau, Fluorescent dyes and their supramolecular host/guest complexes with macrocycles in aqueous solution, *Chem. Rev.* 111 (2011) 7941–7980.
- [35] Z.R. Grabowski, K. Rotkiewicz, W. Rettig, Structural changes accompanying intramolecular electron transfer: focus on twisted intramolecular charge-transfer states and structures, *Chem. Rev.* 103 (2003) 3899–4031.
- [36] (a) S.S. Pasha, H.R. Yadav, A.R. Choudhury, I.R. Laskar, Synthesis of an aggregation-induced emission (AIE) active salicylaldehyde based Schiff base: study of mechanoluminescence and sensitive Zn(II) sensing, *J. Mater. Chem. C Mater. Opt. Electron. Devices* 5 (2017) 9651–9658;  
(b) J. Yang, Y. Gao, T. Jiang, W. Liu, C. Liu, N. Lu, B. Li, J. Mei, Q. Peng, J. Hua, Substituent effects on the aggregation-induced emission and two-photon absorption properties of triphenylamine–dibenzo[a,c]phenazine adducts, *Mater. Chem. Front.* 1 (2017) 1396–1405;  
(c) W. Yang, C. Liu, Q. Gao, J. Du, P. Shen, Y. Liu, C. Yang, A morphology and size-dependent ON-OFF switchable NIR-emitting naphthothiazolium cyanine dye: AIE-active CIEE effect, *Opt. Mater. (Amst)* 66 (2017) 623–629.
- [37] (a) Y. Kang, Y. Yang, L.C. Yin, X. Kang, G. Liu, H.M. Cheng, An amorphous carbon nitride photocatalyst with greatly extended visible-light-responsive range for photocatalytic hydrogen generation, *Adv. Mater.* 27 (2015) 4572–4577;  
(b) R. Saravanan, J. Aviles, F. Gracia, E. Mosquera, V.K. Gupta, Crystallinity and lowering band gap induced visible light photocatalytic activity of TiO<sub>2</sub>/CS (Chitosan) nanocomposites, *Int. J. Biol. Macromol.* 109 (2018) 1239–1245;  
(c) M. Imran, A. Saleem, N.A. Khan, A.A. Khurram, N. Mehmood, Amorphous to crystalline phase transformation and band gap refinement in ZnSe thin films, *Thin Solid Films* 648 (2018) 31–38.
- [38] K. Sattler, The energy gap of clusters, nanoparticles, and quantum dots, handbook of thin films, in: H.S. Nalwa (Ed.), *The Energy Gap of Clusters, Nanoparticles, and Quantum Dots*, Pub. Elsevier, Maryland Heights, 2002p. 61–97.
- [39] (a) S. Wang, R. Tan, Y. Li, Q. Li, S. Xiao, Solid state emission and mechanochromic luminescence of boron 2-(2-pyridyl)imidazole complexes, *Dyes Pigm.* 132 (2016) 342–346;  
(b) P. Xue, B. Yao, J. Sun, Q. Xu, P. Chen, Z. Zhang, R. Lu, Phenothiazine-based benzoxazole derivatives exhibiting mechanochromic luminescence: the effect of a bromine atom, *J. Mater. Chem. C Mater. Opt. Electron. Devices* 2 (2014) 3942–3950.
- [40] (a) L. Pan, Y. Cai, H. Wu, F. Zhou, A. Qin, Z. Wang, B.Z. Tang, Tetraphenylpyrazine-based luminogens with full-colour emission, *Mater. Chem. Front.* 2 (2018) 1310–1316;  
(b) W. Li, L. Wang, J.P. Zhang, H. Wang, Bis-pyrene-based supramolecular aggregates with reversibly mechanochromic and vapochromic responsiveness, *J. Mater. Chem. C Mater. Opt. Electron. Devices* 2 (2014) 1887–1892;  
(c) X. Song, H. Yu, X. Yan, Y. Zhang, Y. Miao, K. Ye, Y. Wang, A luminescent benzothiadiazole-bridging bis(salicylaldehyde)zinc(II) complex with mechanochromic and organogelation properties, *Dalton Trans.* 47 (2018) 6146–6155.
- [41] T. Seki, M. Jin, H. Ito, Introduction of a biphenyl moiety for a solvent-responsive aryl gold(I) isocyanide complex with mechanical reactivation, *Inorg. Chem.* 55 (2016) 12309–12320.
- [42] Y. Cheng, X. Zhang, C. Fang, J. Chen, Z. Wang, Discoloration mechanism, structures and recent applications of thermochromic materials via different methods: a review, *J. Mater. Sci. Technol.* 34 (2018) 2225–2234.
- [43] (a) Y.B. Gong, P. Zhang, Y. Gu, J.Q. Wang, M.M. Han, C. Chen, X.J. Zhan, Z.L. Xie, B. Zou, Q. Peng, Z.G. Chi, Z. Li, The influence of molecular packing on the emissive behavior of pyrene derivatives: mechanoluminescence and mechanochromism, *Adv. Opt. Mater.* 6 (1800198) (2018);  
(b) S.M. Bonesi, R. Erra-Balsells, Electronic spectroscopy of carbazole and N- and C-substituted carbazoles in homogeneous media and in solid matrix, *J. Lumin.* 93 (2001) 51–74;  
(c) E.J. Bowen, E. Mikiewicz, Fluorescence of solid anthracene, *Nature* (159) (1974) 706;  
(d) D.S. McClure, First singlet-singlet electronic transition in the phenanthrene molecule and the band structure of the phenanthrene crystal, *J. Chem. Phys.* 25 (1956) 481–485.
- [44] (a) S. Mecozzi, A.P. West, D.A. Dougherty, Cation- $\pi$  interactions in aromatics of biological and medicinal interest: electrostatic potential surfaces as a useful qualitative guide, *Proc. Natl. Acad. Sci. U.S.A.* 93 (1996) 10566–10571;  
(b) S.L. Cockroft, C.A. Hunter, K.R. Lawson, J. Perkins, C.J. Urch, Electrostatic control of aromatic stacking interactions, *J. Am. Chem. Soc.* 127 (2005) 8594–8595;  
(c) B.W. Gung, J.C. Amicangelo, Substituent effects in C<sub>6</sub>F<sub>6</sub>-C<sub>6</sub>H<sub>5</sub>X stacking interactions, *J. Org. Chem.* 71 (2006) 9261–9270.
- [45] (a) T. Chen, S. Yang, J. Chai, Y. Song, J. Fan, B. Rao, H. Sheng, H. Yu, M. Zhu, Crystallization-induced emission enhancement: a novel fluorescent Au-Ag bimetallic nanocluster with precise atomic structure, *Sci. Adv.* 3 (2017) e1700956;  
(b) Y. Dong, J.W.Y. Lam, A. Qin, Z. Li, J. Sun, H.H.Y. Sung, L.D. Williams, B.Z. Tang, Switching the light emission of (4-biphenyl)phenyldibenzofulvene by morphological modulation: crystallization-induced emission enhancement, *Chem. Commun. (Camb.)* 0 (2007) 40–42.
- [46] (a) U.K. Das, S. Banerjee, P. Dastidar, Primary ammonium monocarboxylate synthesis in designing supramolecular gels: a new series of chiral low-molecular weight gelators derived from simple organic salts that are capable of generating and stabilizing gold nanoparticles, *Chem. Asian J.* 8 (2013) 3022–3031;  
(b) U.K. Das, D.R. Trivedi, N.N. Adarsh, P. Dastidar, Supramolecular synthons in noncovalent synthesis of a class of gelators derived from simple organic salts: instant gelation of organic fluids at room temperature via in situ synthesis of the gelators, *J. Org. Chem.* 74 (2009) 7111–7121.
- [47] (a) S. Marullo, M. Feroci, R. Noto, F. D'Anna, Insights into the anion effect on the self-assembly of perylene bisimide diimidazolium salts, *Dyes Pigm.* 146 (2017) 54–65;  
(b) F. Billeci, F. D'Anna, I. Chiarotto, M. Feroci, S. Marullo, The anion impact on the self-assembly of naphthalene diimide diimidazolium salts, *New J. Chem.* 41 (2017) 13889–13901.
- [48] (a) C. Chen, M. Cheng, H. Li, F. Qiao, P. Liu, H. Li, L. Kloo, L. Sun, Molecular engineering of ionic type perylenediimide dimer-based electron transport materials for efficient planar perovskite solar cells, *Mater Today Energy* 9 (2018) 264–270;  
(b) M. Cheng, K. Aitola, C. Chen, F. Zhang, P. Liu, K. Sveinbjörnsson, Y. Hua, L. Kloo, G. Boschloo, L. Sun, Acceptor–Donor–Acceptor type ionic molecule materials for efficient perovskite solar cells and organic solar cells, *Nano Energy* 30 (2016) 387–397.
- [49] Y. Huang, G. Zhang, F. Hu, Y. Jin, R. Zhao, D. Zhang, Emissive nanoparticles from pyridiniumsubstituted tetraphenylethylene salts: imaging and selective cytotoxicity towards cancer cells in vitro and in vivo by varying counter anions, *Chem. Sci.* 7 (2016) 7013–7019.
- [50] (a) G. Zhang, X. Zhang, L. Kong, S. Wang, Y. Tian, X. Tao, J. Yang, Anion-controlled dimer distance induced unique solid-state fluorescence of cyano substituted styrene pyridinium, *Sci. Rep.* 6 (37609) (2016);  
(b) N. Zhao, J.W.Y. Lam, H.H.Y. Sung, H.M. Su, I.D. Williams, K.S. Wong, B.Z. Tang, Effect of the counterion on light emission: a displacement strategy to change the emission behaviour from aggregation-caused quenching to aggregation-induced emission and to construct sensitive fluorescent sensors for Hg<sup>2+</sup> detection, *Chem. Eur. J.* 20 (2014) 133–138.
- [51] (a) N. Tohnai, M. Sugino, Y. Araki, K. Hatanaka, I. Hisaki, M. Miyata, A facile and versatile approach to efficient enhancement of solid-state luminescence by organic–inorganic hybrid salts, *Dalton Trans.* 42 (2013) 15922–15926;  
(b) M. Sugino, Y. Araki, K. Hatanaka, I. Hisaki, M. Miyata, N. Tohnai, Elucidation of anthracene arrangement for excimer emission at ambient conditions, *Cryst. Growth Des.* 13 (2013) 4986–4992.
- [52] (a) A. Corma, M.S. Galletero, H. García, E. Palomares, F. Rey, Pyrene covalently anchored on a large external surface area zeolite as a selective heterogeneous sensor for iodide, *Chem. Commun. (Camb.)* 0 (2002) 1100–1101;  
(b) P.C. Xue, P. Wang, P. Chen, B. Yao, P. Gong, J. Sun, Z. Zhang, R. Lu, Bright persistent luminescence from pure organic molecules through a moderate intermolecular heavy atom effect, *Chem. Sci.* 8 (2017) 6060–6065.